Fine Chemical Engineering
https://ojs.wiserpub.com/index.php/FCE/

Research Article

Zinc Oxide Films Deposited on ITO Through Electrophoresis

Vanja Fontenele Nunes[1*], Paulo Herbert França Maia Júnior[2], Francisco Marcone Lima[3], João Pedro Santana Mota[3], Francisco Nivaldo Aguiar Freire[3], Antônio Sérgio Bezerra Sombra[1]

[1]Laboratory of Telecommunications and Science and Engineering Materials, Department of Physics, Federal University of Ceará, 60440900, UFC, Fortaleza, Ce, Brazil
[2]Department of Engineering and Materials Science, Federal University of Ceará, 60440554, UFC, Fortaleza, Ce, Brazil
[3]Laboratory of Thin Films and Renewable Energy, Department of Mechanical Engineering, Federal University of Ceará, 60455760, UFC, Fortaleza, Ce, Brazil
E-mail: vanja@alu.ufc.br

Received: 19 May 2025; **Revised:** 4 July 2025; **Accepted:** 10 July 2025

Abstract: Films are materials deposited in nanoscale and macroscale thicknesses applied in different fields, like energy harvesting, solar cells, batteries, capacitors, or gas sensors. There are many ways to synthesize and deposit films on conductive glass, such as indium tin oxide or fluorine tin oxide. Some methods can use high temperatures, vacuum, additives, or applied potentials. Electrophoresis can deposit films of various thicknesses with high quality. This work deposited zinc oxide films on conductive glass made of indium tin oxide for testing as solar cell photoanodes. The deposition used an electrophoretic cell, with a difference in electrical potential between 30 and 50 V for 5 minutes. The thickness of the films varied between 18 and 87 μm. The band gap increased with more material deposited on the glass, from 3 to 4 eV. The results show high crystalline quality, a size range from 30 to 40 nm, absorbance in the ultraviolet range, and a current density of around 2.5 mA/cm^2 when depositing at 30 V for 5 minutes using the electrophoresis methodology. The aim of this study was to develop a cost-effective method to produce semiconductors for applications, such as solar cells.

***Keywords*:** electrophoresis, indium tin oxide, zinc oxide, solar cells

1. Introduction

Nowadays, semiconductors are a key material in different areas, such as sensors, batteries, supercomputers, solar cells, and many others. Solar cells function using the photovoltaic effect, that is, the absorption of photons into the conduction band of the semiconductor, causing a *p*-*n* junction in the material, such as happens to silicon.[1] Other semiconductors are being investigated as a replacement for silicon mono- and polycrystalline, such as CdTe thin films, organic flexible solar cells, dye solar cells, tandem structures, and perovskite, amongst others.[2-4] It is a vast research scenario, with many new materials being tested constantly.

For dye solar cells, the semiconductor that absorbs the photon excited from the dye can be TiO_2, ZnO, or Al_2O_3.[5,6] The electron process inside the cell involves the steps: photoexcitation of the dye molecule, transport from the semiconductor through the external circuit, and dye regeneration from the electrolyte. Any recombination between these steps, whether dye/electrolyte or semiconductor/dye, can reduce the photoelectric conversion.[7] Some of the electrolytes

DOI: https://doi.org/10.37256/fce.6220257263

can be iodide, acetonitrile, glycol, and iodine redox. The counter electrodes are platinum and carbon-based, such as graphene.[7]

The optical, structural, and electronic properties of the applied oxide must be such as a wide band gap, around 3.5 eV, good chemical stability, and high electrical conductivity, so the material can be used for solar cells without deterioration for longer periods of time, making the investment into photovoltaic energy can be more cost effective. One of the factors that can influence the cost of the final device is the synthesis methodology for the semiconductor, which must be easy to manipulate, effective, and produce good crystalline films. One of the advantages of zinc oxide is the possibility of being synthesized using diverse methods, such as spin coating, hydrothermal, sputtering, and vacuum, that is, it can be a very simple, easy cost-balance method or something much more expensive and complex.[8-10] Also, it can be formed as nanotubes, flowers, nanorods, or nano cubes, making it a very flexible material. Another essential component of the Dye-Sensitized Solar Cell (DSSC) is the N719 dye, which absorbs the photon excited by the light. Ruthenium-based dyes are usually used for the Gratzel cell, due to their properties such as chemical stability and efficiency. There are some researchers trying to substitute the ruthenium dyes types (N719, N3, Z907) for more environmentally friendly types, such as dyes from fruits.[11-13] This present study focused on the synthesis of the semiconductor films, and then it opted to use the more established type of dye.

The authors are investigating efficient and simple methods to fabricate solar cells, specifically dye solar cells, with semiconductors like ZnO and SnO_2. Electrophoresis is such a method,[14] and it is the one used in this work to produce good quality crystalline films of zinc oxide on indium tin oxide conductive glass. The films produced were tested for photovoltaic applications, specifically in dye solar cells. The novelty of this work is the coupling of electrophoresis deposition method with ZnO/Indium Tin Oxide (ITO) films.

2. Methodology

The films of zinc oxide were deposited on ITO using a voltage source (K33-300 V, Kasvi) at 30 V, 40 V, and 50 V, each applied for a period of 5 minutes. The solution used for the deposition contained zinc oxide at 8 g/L, dissolved in ethanol. The zinc oxide solution was treated with ultrasound for 15 minutes. The ITO conductive glass was cleaned with distilled water for 15 minutes using ultrasound, before being used in the electrophoresis cell. The zinc oxide powder (purchased from Vetec Ltda., 99% purity, molecular weight 81.37 g/mol, melting point 1,975 °C) was used as-received without further purification. The applied potentials were chosen according to previous work by Nunes et al.,[15] who applied the same potentials and time, but using Fluoride Tin Oxide (FTO) instead of ITO.[16] During the electrophoresis, the ITO served as the negative electrode and platinum as the positive electrode. The formed films were annealed at 450 °C for 30 minutes. For the characterization of the ZnO/ITO films, the X-ray analysis was performed in the 20 to 70° range (Rigaku with CuKα radiation). The results from the X-ray diffraction were used to calculate the grain size, peak positions, and intensities. Ultraviolet-Visible (UV-Vis) analysis was performed to determine the absorption profile of the synthesized films, and the Kubelka-Munk plot was used to estimate the band gap of the films (Evolution One, Thermo Scientific). The I-V plots were obtained using a PGSTAT302N (Metrohm Autolab) under illumination of 100 mW/cm^2. After deposition and characterization, dye solar cells were tested at opposite time frames (2 and 24 h) to characterize the current density produced when the films were used as photoanodes. The assembly of the cells was completed following the methodology of Nunes et al.[17] Each cell had an area of 0.25 cm^2. Figure 1 below shows the sequence of the steps employed in this work.

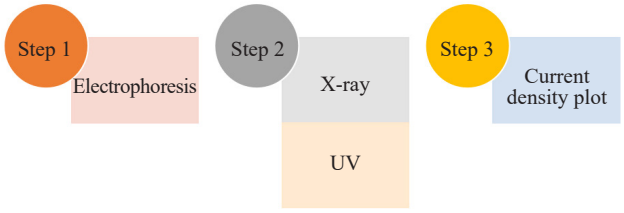

Figure 1. Study fluxogram

The DSSCs were assembled in sandwich mode, with the zinc oxide on ITO film covered in dye as the photoanode, the platinum electrode from Solaronix as the counter electrode, and the iodolyte (also from Solaronix) injected through holes in the platinum electrode. The N719 dye was also purchased from Solaronix. All cell components were used as purchased, except the ZnO film synthesized on the ITO glass by the researchers through electrophoresis.

3. Results and discussion

3.1 *X-ray diffractometer analysis*

The peaks were analysed through an X-Ray Diffractometer (XRD) (Figure 2), and peaks and positions were listed in Table 1. The 30 V film corresponded to ICSD 065122 hexagonal zinc oxide. The 40 V film was ICSD number 065119, also hexagonal form, as the 50 V film with COD 9011599. Table 2 has the peaks and positions for the In_2O_3 found for the films. The ITO peaks were similar to those reported by Abreu et al.[18]

Table 1. Positions of the ZnO peaks

30 V		40 V		50 V	
(hkl)	Pos (°)	(hkl)	Pos (°)	(hkl)	Pos (°)
100	36.88	100	37.16	100	37.07
002	40.09	002	40.34	002	40.21
101	42.18	101	42.48	101	42.37
102	55.6	102	56.01	102	55.84
110	66.46	110	66.99	110	66.82

Table 2. Positions of the In_2O_3 peaks

30 V		40 V		50 V	
(hkl)	Pos (°)	(hkl)	Pos (°)	(hkl)	Pos (°)
222	35.30	222	35.87	222	35.87
441	59.96	044	59.87	044	59.87

The identified peaks for the ZnO films were the same as observed in the study by Torchynska et al.,[19] which analyzed the ZnO doped films at 400 °C, also deposited on Transparent Conductive Oxide (TCO) using spray pyrolysis. The grain size was calculated using the Scherrer method. The Scherrer method calculated the grain size using the $\beta \times \cos\theta$, in the following equation, where D is the grain size (nm); K is the 0.9 constant, and λ is 1.5406.[20]

$$D = \frac{K \times \lambda}{\beta \times \cos\theta} \quad (1)$$

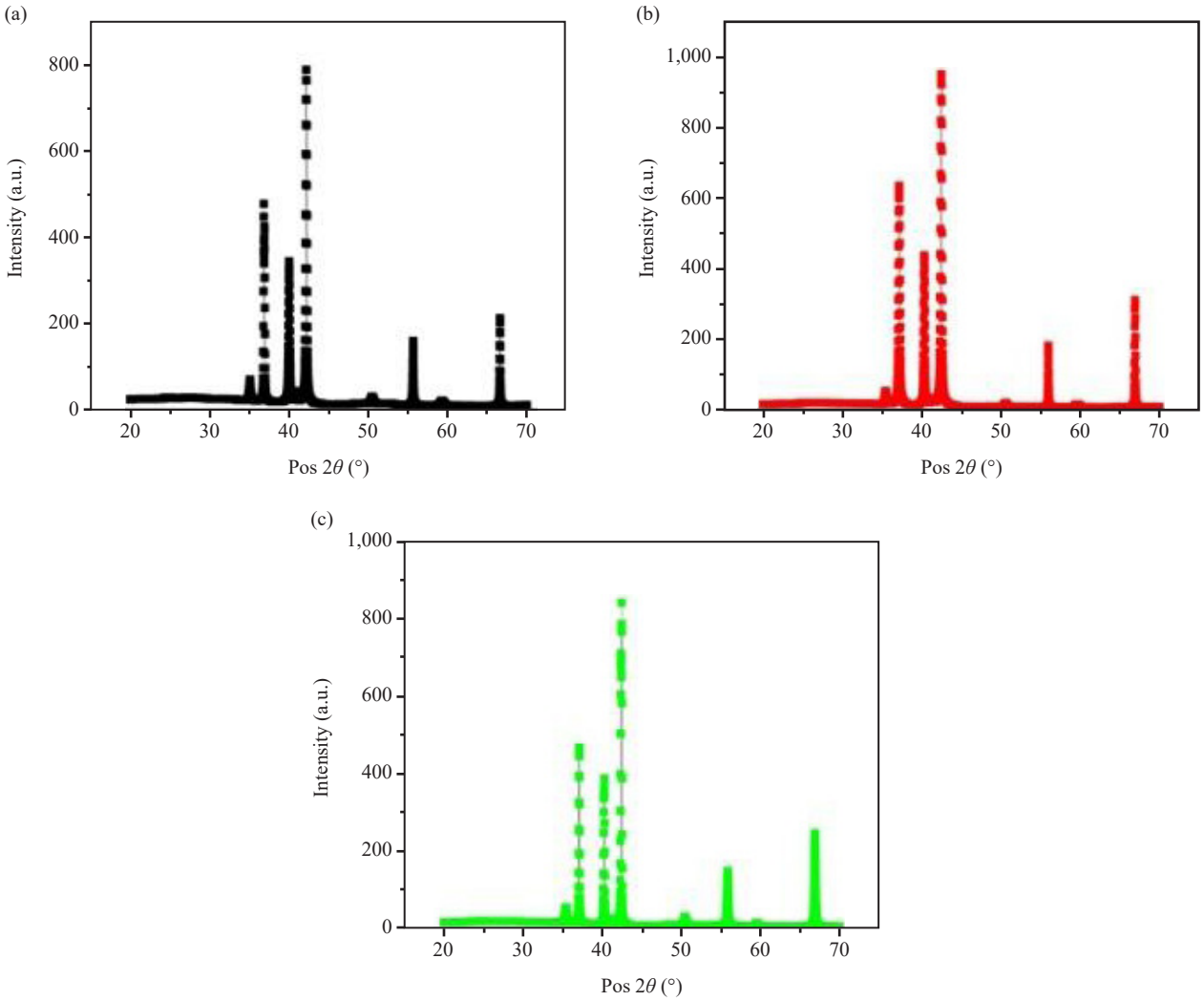

Figure 2. XRD peaks for the ZnO/ITO (a) 30 V, (b) 40 V, (c) 50 V

As listed in Table 3, the grain size for 30 V was 32.72 nm, 33.53 nm for 40 V, and for 50 V, it was equal to 44.18 nm. As expected, more voltage applied to the solution resulted in more material deposited on the film, and the grain size increased from 32.72 to 44.18 nm, an increase of 35% with 20 V more applied to the ITO glass. The high crystallite size can also be explained by the high annealing temperature of 450 °C. The smaller grain size favours a higher surface area and also higher dye loading, which can help to explain the higher current observed for the 30 V deposited film.[21] The dislocation density (δ) and the number of crystallites per unit area (N) were calculated through equations (2) and (3).[21] The values for dislocation density (lines/nm^2) were for 30, 40 and 50, respectively: 9.3×10^{-4}, 8.9×10^{-4} and 5.12×10^{-4}, and the N (nm^{-2}) values were: 0.52; 0.88; and 1.01. The N numbers had a steady growth with more potential applied.[22] The dislocation density decreased, following a more robust crystallite formed by the Electrophoretic Deposition (EPD) process.

$$\delta = \frac{1}{D^2} \tag{2}$$

$$N = \frac{t}{D^3} \tag{3}$$

Table 3. Parameters for the ZnO/ITO

Parameters	30 V	40 V	50 V
a (Å)	2.67	3.2417	2.67
b (Å)	2.67	3.2417	2.67
c (Å)	4.966	5.1876	4.966
Density (g/cm^3)	7.08	5.72	7.08
Cell volume	30.66	47.21	30.66
D (nm) (W-H)	32.72	33.53	44.18

3.2 *Scanning electron microscope analyses*

The Scanning Electron Microscope (SEM) was used to see the formation of the films, as in Figures 3, 4, and 5. The scales used were 3 μm. All the films showed aggregation of 3D forms, such as cubes or tubes, but not predominantly one. These aggregations can help to explain the low efficiency, as they can create more resistance to the electron flow of the dye excited photon, reducing the incident photon current conversion efficiency for the tested cells. Also, the lower sensitization time, 2 hours, is also more favourable for packed formations, such as these.

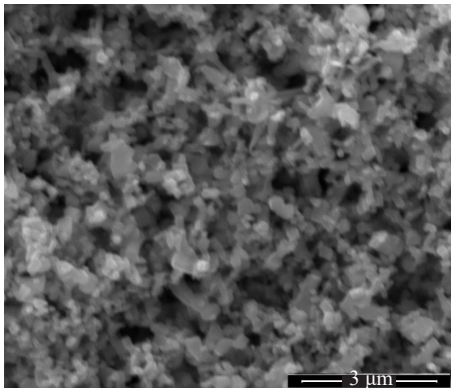

Figure 3. SEM image of the ZnO at 30 V

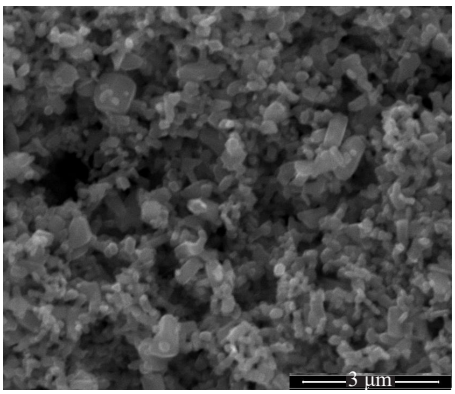

Figure 4. SEM image of the ZnO at 40 V

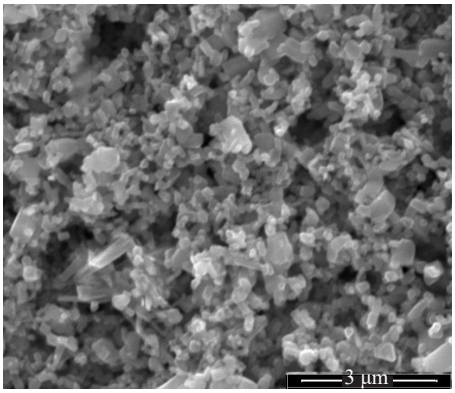

Figure 5. SEM image of the ZnO at 50 V

As the voltage goes from 30 to 50 V, the 3D structures become more visible and brighter. The SEM analyses also made it possible to measure the thickness of the films (Figure 6). For the ZnO film deposited at 30 V, the thickness was around 18.06 µm; for the 40 V deposition film, the value was 33.29 µm, and for the 50 V deposition, the film's thickness was 87.27 µm. The increase in potential also increased the deposited mass on the glass, as expected. The increase in thickness can also account for a higher band gap. The authors also obtained thicknesses for films at 200 °C and 300 °C, around 49 to 55 µm for WS_2 deposited using Radio Frequency (RF) magnetron sputtering. As they treated the films from 25 °C to 300 °C, the thickness went from 22 to 55.08 µm.[23] This work is treated at 450 °C.

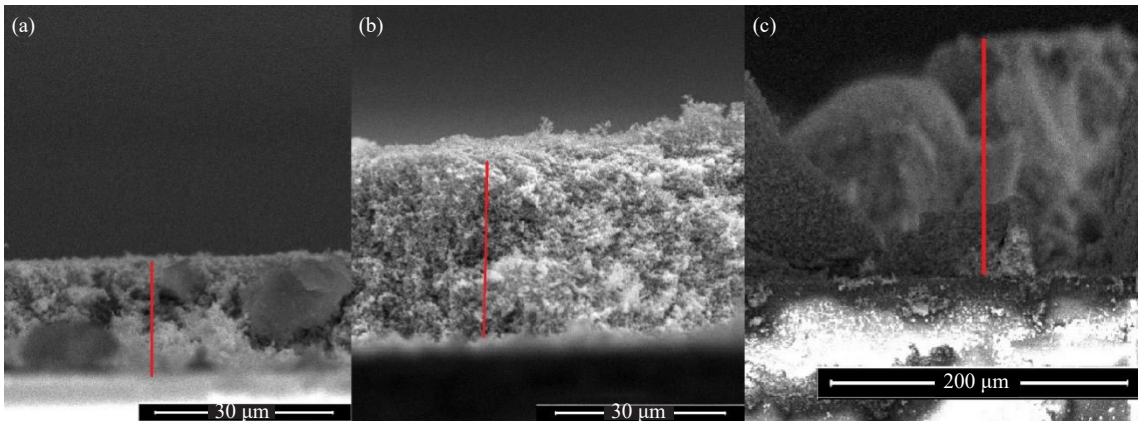

Figure 6. Thickness (a) 30 V, (b) 40 V, (c) 50 V

3.3 *Ultraviolet-visible analyses*

Figure 7 shows the absorbance values for the deposited films. The higher voltage, 50 volts, had the film with the highest peak in the ultraviolet, around 300 nm. The band gap values are listed in Table 4, according to the Kubelka-Munk function (Figure 8). This relation approximates the absorption coefficient with the reflectance values of the film. It is an alternative to the Tauc relation, and is often used to calculate the band gap relations of semiconductors. It uses the absorption coefficient according to equation (4):[24]

$$F(R) \cong \alpha \cong \frac{K}{S} = \frac{(1-R)^2}{2 \times R} \quad (4)$$

Where K is the absorption and S is the scattering coefficients. Using this relation, band gap is calculated using equation (5):

$$(F(R)(hv))^{1/n} = A(hv - E_g) \quad (5)$$

Where hv is the photon energy, A is the constant, and E_g is the band gap. The band gap values of 3.05 and 3.07 eV were close to the ones found by Etefa et al.[6] using incorporated nanoparticles of ITO in ZnO. The band gap value found of 4 eV was close to that reported by Sahoo et al.,[25] who observed ITO band gap values from 4.39 to 4.2 eV. The same absorbance behaviour was observed for the treatment of ITO from 400 °C to 800 °C.[25]

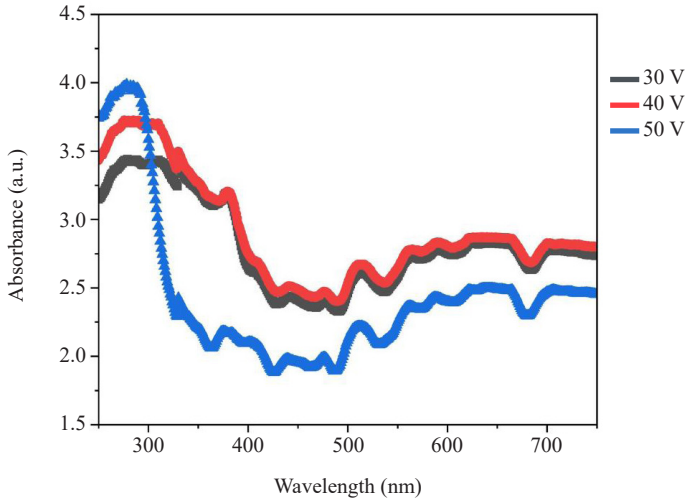

Figure 7. Absorbance

The band gap values represent the distance measured in energy between the highest occupied electronic band of the semiconductor and the lowest unoccupied electronic band of the semiconductor. This distance, in semiconductors, is between the metallic conduction materials and the insulating materials. For the electron to make the leap between the two bands, it is necessary to absorb a "package" of energy, the light photon, that has to contain at least the same amount of energy as the band gap, so that the electron transfer inside the structure can happen and the photocurrent can flow through the system. In semiconductors, one way of changing this value is by doping the oxide with either an element of the *n*-type (excess of electrons in the external layer) or a *p*-type element (excess of holes in the electronic structure). The addition of dopants or impurities increases the electronic density, decreasing the band gap.[26] Figure 9 shows the variation in the thickness and band gap with the applied potential (30, 40, and 50 V). It is possible to observe that both the E_g and the dimension of the film increase together.

Table 4. Band gap values

Applied voltage (V)	Band gap (eV)	Thickness (μm)
30	3.07	18.06
40	3.05	33.29
50	4.03	87.27

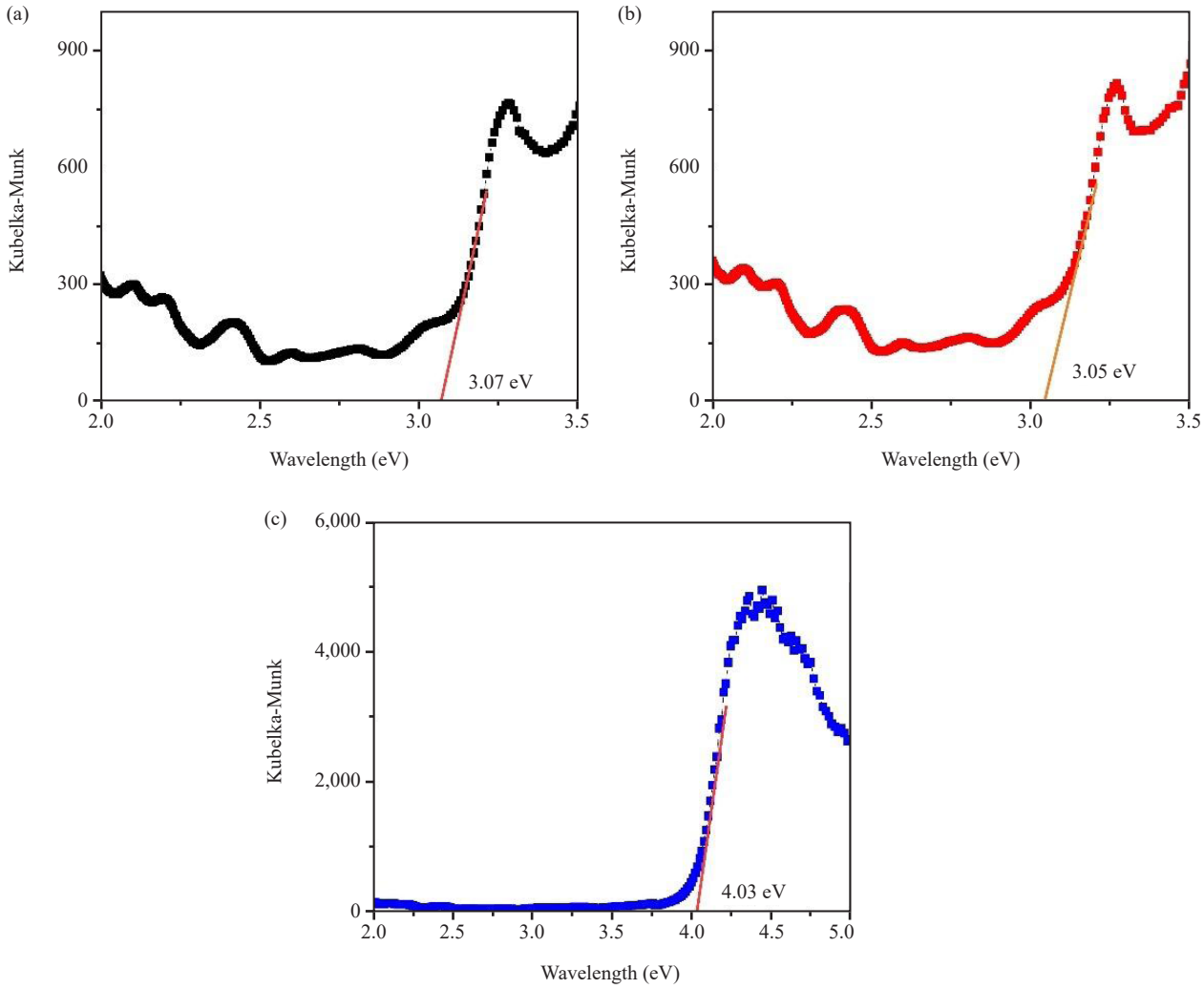

Figure 8. Kubelka-Munk relations (a) 30 V, (b) 40 V, (c) 50 V

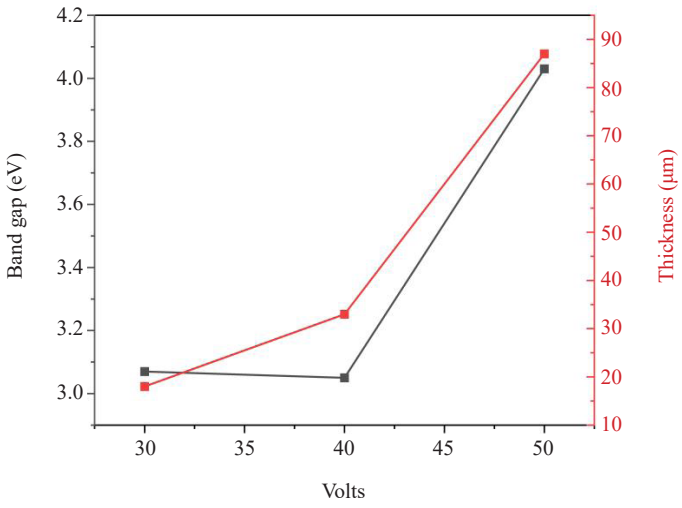

Figure 9. Variation of band gap and thickness corresponding to volts applied

3.4 *Photoanode studies*

The zinc oxide deposited on the ITO was tested for photovoltaic activity, as shown in Figures 10, 11, and 12 and Table 5. The results showed low values for efficiency, mainly due to the high recombination rate indicated by the Fill Factor (FF) values; the highest value for current density (*J*) was for the zinc oxide deposited on the conductive glass at 30 V, with 5 minutes of deposition and 2 hours of immersion dye time. The highest open circuit voltage was found for the film deposited at 50 V for 5 minutes and 24 hours of immersion dye time. The ruthenium-based dye (N719) was chosen due to its high stability and frequent use in dye-sensitized solar cells. The testing was performed after 2 and 24 hours of immersion in the dye to determine which time period would be more suitable for the tests, whether longer or shorter periods.

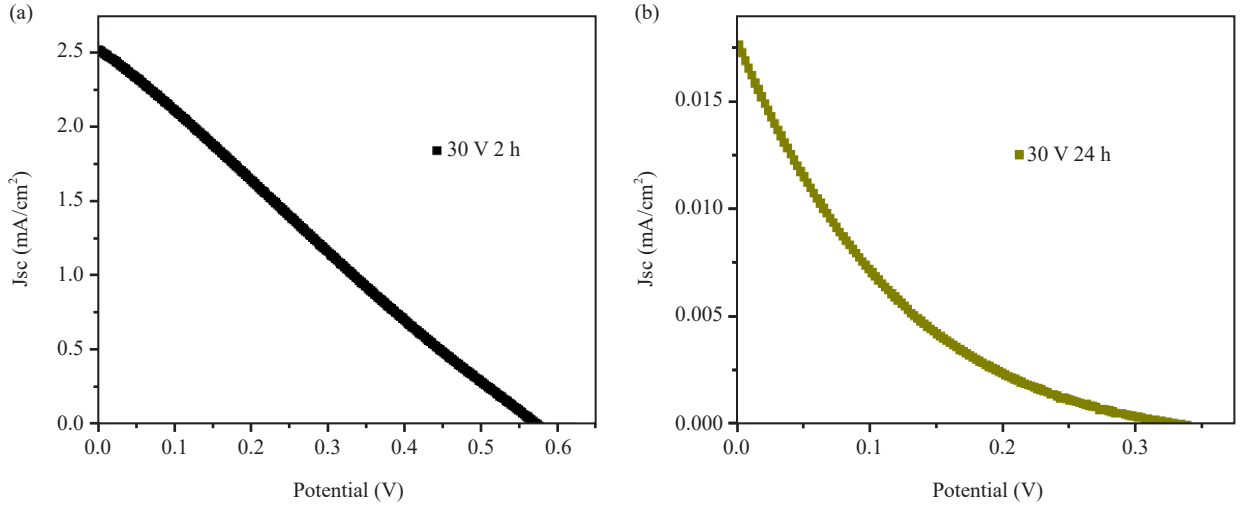

Figure 10. Current density for the 30 V (a) 2 hours, (b) 24 hours of immersion in the dye

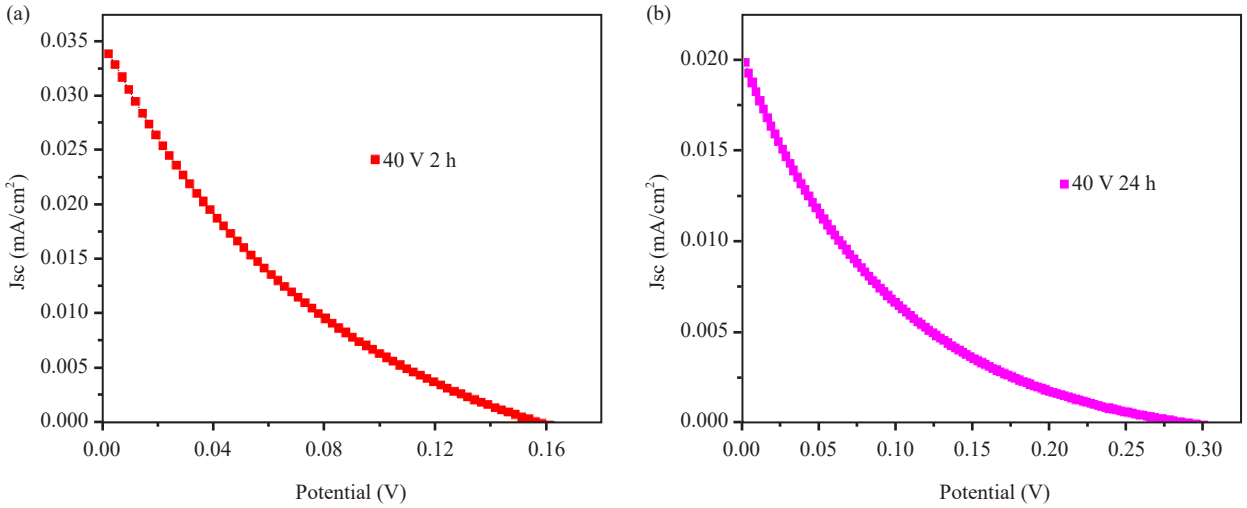

Figure 11. Current density for the 40 V (a) 2 hours, (b) 24 hours of immersion in the dye

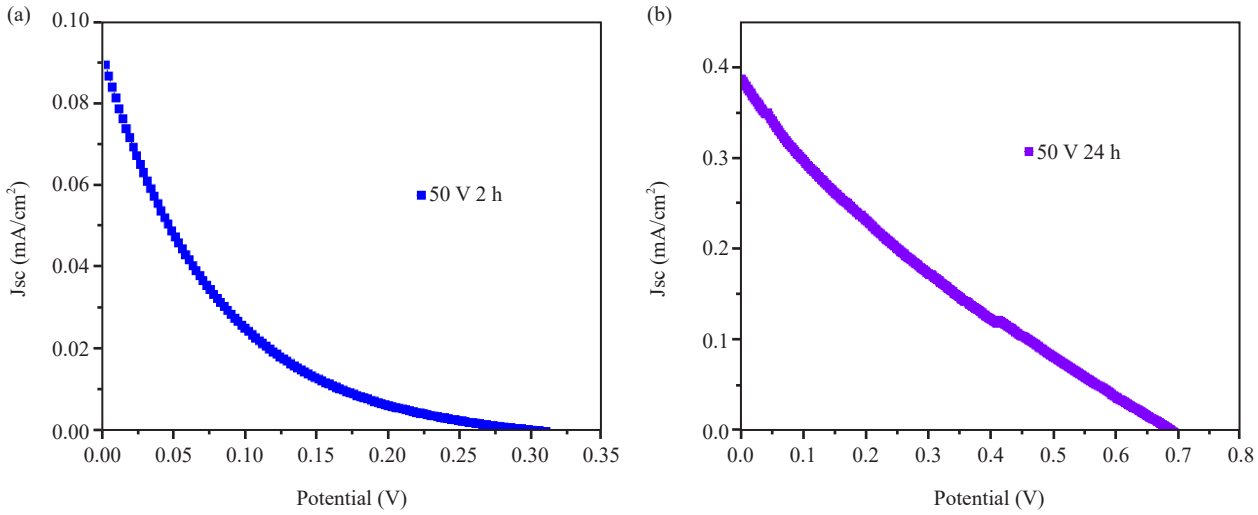

Figure 12. Current density for the 50 V (a) 2 hours, (b) 24 hours of immersion in the dye

Table 5. Photovoltaic values

Parameters	30 V		40 V		50 V	
Immersion time in the dye (h)	2 h	24 h	2 h	24 h	2 h	24 h
J_{max} (mA/cm^2)	2.5	0.017	0.033	0.02	0.089	0.39
R_s (kΩ)	0.241	40,889	7,211	33,090	11,159	4,832
R_{sh} (kΩ)	0.234	9,295	2,678	6,442	1,244	1,365
V_{oc}	0.58	0.34	0.16	0.3	0.32	0.68
FF	0.24	0.12	0.15	0.11	0.09	0.19
η (%)	0.35	0.0008	0.0008	0.0006	0.002	0.052

From the values obtained, the ITO showed better efficiency at short periods of immersion time and lower applied potential, which indicates that future work could focus on lower applied potentials, such as 5, 10, or 20 V, and the same amount of immersion time. The open-circuit voltage (V_{oc}) was lower than that usually found when using zinc oxide deposited on Fluorine Tin Oxide (FTO) conductive glass. The V_{oc} values were comparable to those of DSSCs using ZnO reported by Rafee et al.[27] The FF factor was low, especially for the 50 V at 2 hours of immersion, suggesting that for higher voltage, the cell needs more dye time for stabilization. The series resistance (R_s) and the shunt resistance also greatly affect the final photovoltaic efficiency values. The R_s and R_{sh} were calculated according to Benghanem et al.,[28] and were found all to be in the kΩ range, which is highly unfavourable to the electron flow in the cell circuit. The photovoltaic results were low due to the new method used to deposit the zinc oxide films. Electrophoresis is still mostly used for biological applications, such as protein mobilization. The authors are investigating a new, cost-effective method to produce high-quality, crystalline films, such as ZnO semiconductors. The authors of this study have produced the films using the electrophoresis deposition method, with Fluorine-doped Tin Oxide (FTO), at the same potentials, 30, 40, and 50 V, and are now testing ITO as the substrate, using it as an *n*-type instead of a *p*-type material.[15,29]

4. Conclusion

This study investigated a simple yet effective methodology for the deposition of oxide films and the application of these films in solar cells, specifically dye-sensitized solar cells. The electrophoresis method was successful in the formation of zinc oxide films on ITO conductive glass. The X-Ray Diffractometer (XRD) revealed good crystalline sizes between 30 and 40 nm, and the peaks were thin, confirming the good quality of the deposited films. The scanning electron microscope revealed a 3D formation and thickness from 18 to 87 µm. The results for absorbance had peaks in the UV region, as expected for zinc oxide, and for the ITO, the film could be used for UV detection. The band gap resulted in a range between 3 and 4 eV, close to the band gap of the N719 ruthenium-based dye, which could explain the low efficiency, due to the high recombination, causing low photoactivity. The results showed that the material can be used as sensors or for small Light-Emitting Diodes (LEDs), like digital watches and calculators. As future work, the values of deposition potential can be changed, as well as the deposition time. Additionally, doping the zinc oxide, with elements such as tin (SnO_2 or $SnCl_2$) or Titanium Oxide (TiO_2) can often increase the current density values of the semiconductor.

Acknowledgments

The authors want to thank the CNPq (Process: 402561/2007-4), edital MCT/CNPq n° 10/2007. Also, the National Council for Scientific and Technological Development (number 32/2023). The authors would like to thank Central Analítica-UFC/CT-INFRA/ MCTI-SISNANO/Pro-Equipamentos CAPES.

Conflict of interest

There is no conflict of interest to declare.

References

[1] Sayed, H.; Ahmed, A. M.; Hajjiah, A.; Aly, A. H.; Omer, A. M.; Osman, M. A. Optimization of amorphous silicon solar cells through photonic crystals for enhanced optical properties. *Sci. Rep*. **2025,** *15*, 16529.

[2] Luo, Y.; Tian, Y.; Zhao, K.; Mao, W.; Liu, C.; Shen, J.; Cheng, Z.; Değer, C.; Miao, X.; Zhang, Z.; et al. Inductive effects in molecular contacts enable wide-bandgap perovskite cells for efficient perovskite/TOPCon tandems. *Nat. Commun*. **2025,** *16*, 4516.

[3] Ying, Z.; Su, S.; Li, X.; Chen, G.; Lian, C.; Lu, D.; Zhang, M.; Guo, X.; Tian, H.; Sun, Y.; et al. Antisolvent seeding of self-assembled monolayers for flexible monolithic perovskite/Cu(In, Ga)Se_2 tandem solar cells. *Nat. Energy* **2025,** *10*, 737-749.

[4] Kondratenko, S. V.; Mykytiuk, A. O. Photoelectric properties of ITO/CdTe/Si heterostructures with nanocrystalline films and a two-dimensional ITO layer. *Opt. Mater*. **2024,** *157*, 116061.

[5] Liu, S.; Xu, X.; Jiang, J. Flexible transparent ITO thin film with high conductivity and high-temperature resistance. *Ceram. Int*. **2024,** *50*, 47649-47654.

[6] Etefa, H. F.; Dejene, F. B. The effect of indium tin oxide nanoparticles (ITO NPs) incorporated with ZnO NPs based on structural, optical and application for flexible dye sensitized solar cells (FDSSCs). *Opt. Mater*. **2024,** *156*, 115962.

[7] Zheng, D.; Yang, X.; Čuček, L.; Wang, J.; Ma, T.; Yin, C. Revolutionizing dye-sensitized solar cells with nanomaterials for enhanced photoelectric performance. *J. Clean. Prod*. **2024,** *464*, 142717.

[8] Yang, F.; Song, J. M.; Chen, X. Y.; Lu, X.; Li, J. H.; Xue, Q. Q.; Han, B.; Meng, X. D.; Li, J. J.; Wang, Y. F. Ultrasonic spray pyrolysis-induced growth of highly transparent and conductive F, Cl, Al, and Ga co-doped ZnO films. *Solar Energy* **2021,** *228*, 168-174.

[9] Li, J.; Li, J.; Ma, N.; Guan, L.; Tan, C.; Xia, Z.; Xu, J.; Zuo, J. Preparation of ZnO/TiO_2 NTs-loaded materials and their photocatalytic performance. *Chem. Phys. Letters* **2024,** *838*, 141084.

[10] Sufyan, M.; Mehmood, U.; Gull, Y. Q.; Nazar, R.; Khan, A. U. H. Hydrothermally synthesize zinc oxide (ZnO) nanorods as an effective photoanode material for third-generation dye-sensitized solar cells (DSSCs). *Mater. Lett*. **2021,** *297*, 130017.
[11] Yahya, M.; Bouziani, A.; Ocak, C.; Seferoğlu, Z.; Sillanpää, M. Organic/metal-organic photosensitizers for dye-sensitized solar cells (DSSC): Recent developments, new trends, and future perceptions. *Dyes Pigm*. **2021,** *192*, 109227-109264.
[12] Girón-Juárez, K. H.; Messina-Fernández, S. R.; Navarro-Santos, P.; Vázquez-Guevara, J. A.; Mendoza-Pérez, R. Natural extracts from Rhus microphylla and Opuntia joconostle as mono and co-sensitizers for efficiency enhancement of nano-TiO_2 based dye-sensitized solar cells. *Optik* **2024,** *306*, 171793-171804.
[13] Nasyori, A.; Patunrengi, I. I.; Noor, F. A. Investigate the utilization of novel natural photosensitizers for the performance of dye-sensitized solar cells (DSSCs). *J. King Saud Univ. Sci*. **2024,** *36*, 103423-103430.
[14] Nunes, V. F.; Maia Júnior, P. H. F.; Almeida, A. F. L.; Freire, F. N. A. EPD method for thin films on solar cells. *Mater. Lett*. **2024,** *358*, 135896.
[15] Nunes, V. F.; Teixeira, E. S.; Maia Júnior, P. H. F.; Almeida, A. F. L.; Freire, F. N. A. Study of electrophoretic deposition of ZnO photoanodes on fluorine-doped tin oxide (FTO) glass for dye-sensitized solar cells (DSSCs). *Cerâm*. **2022,** *68*, 120-125.
[16] Holzhey, P.; Prettl, M.; Collavini, S.; Mortan, C.; Saliba, M. Understanding the impact of surface roughness: changing from FTO to ITO to PEN/ITO for flexible perovskite solar cells. *Sci. Rep*. **2023,** *13*, 6375.
[17] Nunes, V. F.; Graça, M. P. F.; Hammami, I.; Almeida, A. F. L.; Freire, F. N. A. Effect of time and voltage on the electrophoresis deposition of zinc oxide thin films for photovoltaic applications. *Appl. Sci*. **2024,** *14*, 1202.
[18] Abreu, I. M. G.; Maia, V. A.; Souza, R. F. B.; Neto, A. O. Synthesis and performance of PdAu/ITO electrocatalysts in urea oxidation reaction. *Int. J. Electrochem. Sci*. **2024,** *19*, 100810.
[19] Torchynska, T.; Filali, B. E.; Garcia, J. O.; Polupan, G.; Espinola, J. L. C. Emission, structure, and electrical characteristics of ZnO nanocrystalline films co-doped with Al and In elements. *Results Opt*. **2025,** *18*, 100773.
[20] Khorashadizade, E.; Nasiri, F. Hydrogenation-driven phase and morphology changes in Ru-Doped TiO_2 nanotubes. *Fine Chemical Engineering* **2025,** *6*(2), 174-185.
[21] Katta, V. S.; Das, A.; Dileep, K. R.; Cilaveni, G.; Pulipaka, S.; Veerappan, G.; Ramasamy, E.; Meduri, P.; Asthana, S.; Melepurath, D.; et al. Vacancies induced enhancement in neodymium doped titania photoanodes based sensitized solar cells and photo-electrochemical cells. *Sol. Energy Mater. Sol. Cells* **2021,** *220*, 110843.
[22] Damgasi, E.; Kartal, E.; Gucluer, F.; Seyhan, A.; Kaplan, Y. Impact of temperature optimization of ITO thin film on tandem solar cell efficiency. *Materials* **2024,** *17*(11), 2784.
[23] Jafari, M.; Shahidi, M. M.; Ehsain, M. H. Effect of substrate temperature on properties of WS_2 thin films. *Sci. Rep.* **2025,** *15*, 21561.
[24] Makula, P.; Pacia, M.; Macyk, W. How to correctly determine the band gap energy of modified semiconductor photocatalysts based on UV-Vis spectra. *J. Phys. Chem. Lett*. **2018,** *9*(23), 6814-6817.
[25] Sahoo, A. K.; Au, W.; Pan, C. Characterization of indium tin oxide (ITO) thin films towards terahertz (THz) functional device applications. *Coatings* **2024,** *14*(7), 895.
[26] Alyami, M.; El-Bashir, S. Enhanced thermal stability photophysical properties of photoselective PMMA/ITO nanohybrid films for greenhouse cooling in hot climates. *J. Saudi Chem. Soc*. **2024,** *28*(6), 101945.
[27] Rafee, V.; Razeghizadeh, A.; Yazdizadeh, F.; Nakhaei, R. Efficiency enhancement of DSSCs based on sol-gel prepared ZnO nanoparticles through cosensitization with natural and synthetic pigments. *Chem. Phys. Impact* **2025,** *10*, 100868.
[28] Benghanem, M. S.; Alamri, S. N. Modeling of photovoltaic module and experimental determination of serial resistance. *J. Taibah Univ. Sci*. **2009,** *2*, 94-105.
[29] Souza, A. P. S.; Oliveira, F. G. S.; Nunes, V. F.; Lima, F. M.; Almeida, A. F. L.; Carvalho, I. M. M.; Graça, M. P. F.; Freire, F. N. A. High performance SnO_2 pure photoelectrode in dye-sensitized solar cells achieved via electrophoretic technique. *Sol. Energy* **2020,** *211*, 312-323.